

# 1 Development, characterization and application of an improved online 2 reactive oxygen species analyzer based on MARGA

3 Jiyao Wu<sup>1,2</sup>, Chi Yang<sup>1,2</sup>, Chunyan Zhang<sup>1,2</sup>, Fang Cao<sup>1,2</sup>, Aiping Wu<sup>1,2</sup>, Yanlin Zhang<sup>1,2</sup>

4 \*

5 <sup>1</sup> Yale-NUIST Center on Atmospheric Environ., Joint International Research  
6 Laboratory of Climate and Environment Change (ILCEC), Nanjing University of  
7 Information Science and Technology, Nanjing 210044, China

8 <sup>2</sup> School of Applied Meteorology, Nanjing University of Information Science and  
9 Technology, Nanjing 210044, China

10 Correspondence: Yanlin Zhang ([zhangyanlin@nuist.edu.cn](mailto:zhangyanlin@nuist.edu.cn))

## 11 Abstract

12 Excessive reactive oxygen species (ROS) in the human body is an important factor  
13 leading to diseases. Therefore, research on the content of reactive oxygen species in  
14 atmospheric particles is necessary. In recent years, the online detection technology of  
15 ROS has been developed. However, there are few technical studies on online detection  
16 of ROS based on the DTT method. Here, to modify the instrument, it is added a DTT  
17 experimental module that is protected from light and filled with nitrogen at the end,  
18 based on the Monitor for AeRosols and Gases in ambient Air (MARGA). The  
19 experimental study found that the detection limit of the modified instrument is 0.024  
20 nmol min<sup>-1</sup>. The DTT consumption rate of blank sample (ultra-pure water) is reduced  
21 by 44 %, which eliminates the influence of outside air and light in the experiment. And  
22 the accuracy of the online instrument is determined by comparing the online and offline  
23 levels of the samples, which yielded good consistency (slope 0.97, R<sup>2</sup>=0.95). It shows  
24 that the performance of the instrument is indeed optimized, the instrument is stable, and  
25 the characterization of ROS is accurate. The instrument not only realizes the online  
26 detection conveniently and quickly, but also achieves the hour-by-hour detection of  
27 ROS based on the DTT method. Meanwhile, reactive oxygen and inorganic ions in  
28 atmospheric particles are quantified using the online technique in the northern suburbs  
29 of Nanjing. It is found that the content of ROS during the day is higher than that at night,  
30 especially after it rains, ROS peaks appear in the two time periods of 08:00-10:00 and  
31 16:00-18:00. In addition, examination of the online ROS and water-soluble ions (SO<sub>4</sub><sup>2-</sup>,  
32 NO<sub>3</sub><sup>-</sup>, NH<sub>4</sub><sup>+</sup>, Na<sup>+</sup>, Ca<sup>2+</sup>, K<sup>+</sup>), BC and polluting gases (SO<sub>2</sub>, CO, O<sub>3</sub>, NO, NO<sub>x</sub>)  
33 measurements revealed that photo-oxidation and secondary formation processes could  
34 be important sources of aerosol ROS. This method breakthrough enables the  
35 quantitative assessment of atmospheric particulate matter ROS at the diurnal scale,  
36 providing an effective tool to study sources and environmental impacts of ROS.

## 37 1、 Introduction

38 Air quality is a major issue affecting human health, and prolonged exposure to  
39 high ambient particulate concentrations can lead to a significant increase in the  
40 probability of respiratory and cardiovascular diseases, which can seriously impair  
41 human health (Delfino et al., 2005; Ghio et al., 2012; Pöschl and Shiraiwa, 2015). The  
42

43 production of reactive oxygen species (ROS) in the human body is the most reliable  
44 pathophysiological mechanism proposed, and excessive reactive oxygen species can  
45 cause an imbalance between the oxidative system and the antioxidant system, causing  
46 oxidative stress and tissue damage (Ahmad et al., 2021; Akhtar et al., 2010; Borm et al.,  
47 2007; Delfino et al., 2013; Lodovici and Bigagli, 2011). Thus, oxidative potential (OP)  
48 has been proposed as a more biologically relevant indicator than particulate matter (PM)  
49 mass concentration to represent the combined effects of multiple toxic components in  
50 PM (Ayres et al., 2008; Hellack et al., 2015; Janssen et al., 2015). Understanding the  
51 generation mechanism and source characteristics of reactive oxygen species is essential  
52 for making reasonable pollution control decisions and reducing their impact on human  
53 health.

54 In recent years, the analysis method of oxidation potential has cell detection and  
55 cell-free detection. To provide a simpler and quicker way to determine the oxidation  
56 potential of environmental particulate matter, cell-free methods such as electron spin  
57 (or paramagnetic) resonance ( $OP_{ESR}$ ), dithiothreitol assay ( $OP_{DTT}$ ), ascorbic acid assay  
58 ( $OP_{AA}$ ), high-performance liquid chromatography (HPLC) and glutathione assay  
59 ( $OP_{GSH}$ ) are often used as the main measurement methods for ROS (Bates et al., 2019;  
60 Ghio et al., 2012). Through the comparison and analysis of these various methods by a  
61 large number of researchers, the DTT method is generally considered to be the most  
62 common and comprehensive method to reflect the magnitude of the chemical oxidation  
63 potential of particulate matter (Hedayat et al., 2014; Xiong et al., 2017).

64 Generally, the cell-free method still has problems with detection delays and  
65 degradation of particulate chemical components during sample storage, which not only  
66 leads to inaccurate detection data, but also the inability to capture daily changes.  
67 Therefore, the development of online detection technology becomes necessary  
68 (Charrier et al., 2016; Dou et al., 2015; Fang et al., 2017; Li et al., 2012; Liu et al., 2014;  
69 Velali et al., 2016; Vreeland et al., 2017). So far, the development of online detection  
70 technology is mainly based on the DCFH method and the DTT method. On the one  
71 hand, an online detection technology based on the DCFH method has been reported  
72 previously (Eiguren-Fernandez et al., 2017; Huang et al., 2016; Sameenoi et al., 2012;  
73 Wragg et al., 2016). However, some researchers believe that in the DCFH method, the  
74 horseradish peroxidase (HRP) will promote the production of hydroxyl free radicals,  
75 leading to an overestimation of ROS content (Pal et al., 2012). On the other hand, based  
76 on the DTT method to develop online detection technology (Fang et al., 2014;  
77 Puthussery et al., 2018), The semi-automatic detection system researched by Fang et al,  
78 based on the DTT method cannot realize an online collection of environmental samples.  
79 On this basis, Puthussery et al used a mist chamber (MC) to continuously collect  $PM_{2.5}$   
80 in environmental water and realized fully automatic hourly ROS detection.

81 However, these detection methods ignore the influence of air and light on the  
82 experiment. As the main reagent of the experiment, dithiothreitol (DTT) and 5,5'-  
83 dithiobis (2-nitrobenzoic acid) (DTNB) are easily oxidized by air (Chen et al., 2010).  
84 We achieve accurate measurement of the oxidation potential of environmental  
85 particulates by shielding from light and filling with nitrogen. In addition, the present  
86 study is developed on the basis of the MARGA, which is a state-of-art instrument.

87 MARGA measures near-real-time water-soluble particulate species and their gaseous  
88 precursors (Chen et al., 2017). MARGA is used to collect particulate matter and is  
89 connected to the optimized DTT<sub>v</sub> detection part to observe the oxidation potential hour  
90 by hour. The system realizes simultaneous observation of oxidation potential and  
91 inorganic ions. Here, we optimize the performance of the instrument and measure the  
92 hourly averaged OP of ambient PM<sub>2.5</sub>. The reliability of online detection of oxidation  
93 potential data is supported by analyzing the correlation between ions, polluting gases,  
94 BC and oxidation potential.

## 95 **2、 Materials and Method**

### 96 **2.1 Instrument set-up and improvement**

97 Figure 1 shows the scheme and schematic diagram of the system for DTT online  
98 detection. The instrument is set up in the Atmospheric Environ. monitoring laboratory  
99 on the roof of the Wende Building of Nanjing University of Information Engineering  
100 (30 m above the ground) and the room temperature is maintained at 20°C. The entire  
101 system is composed of the MARGA, the automatic sample-receiving device, and the  
102 DTT experimental reaction device. The MARGA is used as an instrument for detecting  
103 atmospheric aerosols and inorganic components of gases (water-soluble ions Cl<sup>-</sup>、NO<sub>3</sub><sup>-</sup>、  
104 SO<sub>4</sub><sup>2-</sup>、NH<sub>4</sub><sup>+</sup>、Na<sup>+</sup>、K<sup>+</sup>、Mg<sup>2+</sup>、Ca<sup>2+</sup>), and it collects gases using a wet rotary separator  
105 and aerosols using steam injection, and absorbs gases and aerosols into the aqueous  
106 phase separately to separate them from each other. Then, the resulting solution is  
107 analyzed by ion chromatography equipped with a conductivity detector. That is, the gas  
108 and aerosol are analyzed separately to detect the gas precursors and different ionic  
109 compositions in the aerosol.

110 In past studies, MARGA was often used to detect the content of inorganic  
111 components of atmospheric aerosols and gases in cities around the world (Rumsey et  
112 al., 2014). And Chen et al. conducted a special evaluation study on the accuracy and  
113 precision of MARGA (Chen et al., 2017). In addition, Stieger et al. achieved  
114 quantitative analysis of low molecular weight organic acids in the atmospheric gas  
115 phase and particle phase by modifying MARGA (Stieger et al., 2019). Hemmilä et al  
116 used a MARGA ligation an electrospray ionization quadrupole mass spectrometer (MS)  
117 to achieve 1-hour resolution quantification of 7 different amines in gas and particulate  
118 phases in forest air in northern Finland. (Hemmilä et al., 2018) As a mature commercial  
119 instrument, MARGA can measure the inorganic components of atmospheric aerosols  
120 and gases with 1-hour resolution. In this study, based on MARGA, the DTT  
121 experimental part is connected to realize the hour-by-hour simultaneous detection of  
122 aerosol inorganic components and ROS.

123 In the DTT reaction module, to avoid the influence of light and air on the  
124 experiment, all pipelines, reaction flasks and mixing flasks are sealed and protected  
125 from light by aluminum foil. The whole DTT experimental part was filled with N<sub>2</sub> by  
126 pump A and pump B before the experiment started. In addition, we added a refrigerator  
127 to store DTT, DTNB and other experimental solutions. During the DTT experiment, the  
128 reaction tube and mixing tube were placed in an incubator at 37°C to simulate the  
129 temperature of human lungs. To realize the subsequent DTT experimental reactions, as

130 in Figure 1 we collected the liquid-phase aerosols into sample tubes through a dual-  
131 channel split-flow controlled-volume peristaltic pump. And set peristaltic pump 1 speed  
132 to  $1.55 \text{ ml h}^{-1}$  to finish  $1.5 \text{ ml h}^{-1}$  sample volume.

133 Finally, the determination of DTT activity is achieved by the continuous regular  
134 operation of the programmable pumps A and B and the detection of the  
135 spectrophotometer. (see Sect. 2.2.1 for details)

## 136 **2.2 Method**

### 137 **2.2.1 Online DTT assay measurement**

138 The whole measurement step is divided into three steps: sample collection, DTT  
139 reaction part, and spectrophotometer detection. In the first step (the sample collection),  
140 the MARGA will discharge 25 ml of aerosol liquid every hour, and use the dual-channel  
141 split flow control volume peristaltic pump 1 to add 1.55 ml of the solution (to ensure  
142 1.5 ml of sample) into the sample tube, and the rest will enter the automatic sampling  
143 device to save through the peristaltic pump 2 (the automatic sampler is set to rotate one  
144 grid per hour).

145 In the second step (the part is protected from light and in a nitrogen environment),  
146 the reaction part is divided into a DTT oxidation step and a DTT determination  
147 step(Wang et al., 2019). First (DTT oxidation step), use pump A to add 5 mL potassium  
148 phosphate buffer ( $0.1 \text{ mol L}^{-1}$ ), 1.5 mL aerosol extract sample, and 0.5 mL DTT ( $1$   
149  $\text{mmol L}^{-1}$ ) into the mixing bottle (MV) in sequence. Inhale ultrapure water to clean the  
150 syringe of pump A. DTT reacts with the aerosol extract in MV. [To adapt to the  
151 experimental process, the concentration and addition volume of each substance are  
152 changed in the experiment, but the concentration of each substance in the mixed  
153 solution is similar to that of Cho et al. \(Cho et al., 2005\). Lin et al. found that the initial  
154 DTT concentration will affect the final  \$\text{DTT}\_v\$  value \(Lin et al., 2019\). During the  
155 experiment, the initial DTT concentration was always kept at 1 mM, so it did not affect  
156 the judgment of the daily change of ROS content.](#)

157 Second (DTT determination step), after completing the first step, at 0.10.20.30.40  
158 minutes, use pump A to draw 1ml mixed solution in the mixing bottle and add it to the  
159 reaction bottle. Then, immediately add 1 mL TCA (10% w/v; quencher) to the reaction  
160 vial (RV, wrapped in aluminum foil to prevent possible light interference) using pump  
161 A. Add 0.05 mL DTNB ( $1 \text{ mmol L}^{-1}$ ) via pump B and mix. The residual DTT reacts  
162 with DTNB to form light absorption product 2-nitro-5-thiobenzoic acid (TNB) with  
163 high extinction performance at 412 nm.

164 In the third step, in the detection part of the spectrophotometer, use pump A to add  
165 4 mL Tris buffer ( $0.4 \text{ mol L}^{-1}$ , containing  $20 \text{ mmol L}^{-1}$  EDTA) into the reaction flask  
166 (RV). After the reaction is completed, use pump A to add the final mixture solution in  
167 the reaction flask to the LWCC for the absorbance test. The data acquisition software  
168 (Spectra Suite) records the absorbance at 412 and 700 nm every 10 min (select the  
169 baseline absorbance of TNB). Then, the system uses deionized water (deionized water)  
170 for self-cleaning to eliminate any residual liquid in the reaction flask, tubing, syringe,  
171 and LWCC. To determine the rate of DTT consumption, the time interval is 10 min, and  
172 a total of 6 (0 min, 10 min, 20 min, 30 min, 40 min, 50 min) data points of DTT

173 concentration over time are generated. Finally, the automated system performs the self-  
174 cleaning procedure again to ensure that there is no residue, and the system repeats the  
175 above operations in the next hour to realize hourly detection of DTT activity.

$$176 \quad \Delta DTT = -\sigma Abs \cdot \frac{N_0}{Abs_0} \quad (1)$$

$$177 \quad DTT_v = \frac{\Delta DTT_s(\text{nmol min}^{-1}) - \Delta DTT_b(\text{nmol min}^{-1})}{V_t(\text{m}^3) \times \frac{V_s(\text{mL})}{V_e(\text{mL})}} \quad (2)$$

178 where  $\sigma Abs$  is the slope of absorbance versus time;  $Abs_0$  is the initial absorbance  
179 calculated from the intercept of the linear regression of absorbance versus time; and  $N_0$   
180 is the initial moles of DTT added in the reaction vial.  $\Delta DTT_s(\text{nmol min}^{-1})$  is the  $DTT_v$   
181 consumption rate of the sample,  $\Delta DTT_b(\text{nmol min}^{-1})$  is the blank DTT consumption  
182 rate,  $V_t(\text{m}^3)$  is the sampling volume corresponding to the sample, and  $V_s(\text{mL})$  is the  
183 injection volume,  $V_e(\text{mL})$  is the sampling volume.

### 184 **2.2.2 Online DTT instrument performance**

185 The performance of the automated system is characterized by testing to determine  
186 the instrument response, limit of detection (LOD), precision and accuracy, while using  
187 a large flow sampler to collect samples for offline and online comparative analysis. (See  
188 Sect.3.1 for details)

189 We perform DTT activity detection and comparison on samples collected by 9,10-  
190 phenanthraquinone (PQN) and offline high-flow samplers. First, we select PQN with  
191 concentrations of 0.01, 0.02, 0.025, 0.05, 0.085  $\text{nmol L}^{-1}$  to compare online and offline  
192 DTT activity detection to determine the error of online and offline experiments. The  
193 details of PQN analysis can be found in Supplement S1. Secondly, select 10 offline  
194 collected samples for online and offline comparison, and then combine the  
195 experimental error between online and offline determined by PQN (PQN online and  
196 offline orthogonal fitting) to analyze the accuracy of online and offline.

### 197 **2.2.3 Instrument maintenance**

198 The MARGA is calibrated using internal and external standards. The internal  
199 standard is a 10  $\text{mg L}^{-1}$  LiBr solution. The external standard calibration is performed  
200 after replacing the anion and cation columns, and the replacement cycle is generally 4  
201 to 5 months. At the same time, the MARGA system is cleaned with 1% hydrogen  
202 peroxide and 10% acetone solution, and the airflow is calibrated every two months. In  
203 the DTT experimental module, DTT and DTNB solutions are prepared every 4 days.  
204 Before each test, perform a comprehensive light and nitrogen bag inspection. To ensure  
205 the accuracy of the experimental data, a standard curve was measured before each  
206 experiment. The instrument pipeline is cleaned once a week, as shown in Figure 1. The  
207 programmable pump A and pump B are connected to the ultrapure water channel.  
208 During the cleaning process, all pipelines, reaction tubes and mixing tubes are cleaned.

### 209 **2.3 Collection and preparation of environmental samples**

210 The sampling point is located on the roof of the seventh floor of the Maintenance  
211 Branch (34°58' N, 117°26' E) of the Power Company, Yunlong District, Xuzhou City.  
212 The surrounding buildings mainly include auto repair shops, logistics centers,  
213 pharmaceutical factories, and large residential areas and farmland. A large flow  $PM_{2.5}$

214 sampler (KC-6120) is used for continuous sampling, and a total of 10 samples are  
215 collected (October 21, 2018-October 31, 2018). When sampling, the flow rate is  $1.0 \text{ m}^3$   
216  $\text{min}^{-1}$ , and each sampling time is 24 h. In this study, we collected samples using quartz  
217 filters and stored them in a refrigerator at  $-26 \text{ }^\circ\text{C}$ . Before the start of the experiment, the  
218 collected samples were subjected to extraction processing, and a sample film with a  
219 diameter of 16 mm is cut into a brown glass bottle, 5 ml ultrapure water is added to  
220 shake for 30 min, and filtered with a  $0.22 \text{ }\mu\text{m}$  PTFE syringe filter to remove insoluble  
221 substances.

## 222 **3. Results and discussion**

### 223 **3.1 Instrument performance**

#### 224 **3.1.1 Improvement of the instrument**

225 As we all know, photo-oxidation promotes the generation of ROS (Fang et al.,  
226 2016; Visentin et al., 2016; Yang et al., 2014). In addition, during the measurement  
227 process, the ingress of air inside the instrument will also cause the DTT activity to  
228 increase. Therefore, before on-site deployment, the online DTT inspection instrument  
229 is optimized by filling in nitrogen gas and shielding the whole from light. And  
230 respectively detect the DTT consumption rate ( $\Delta\text{DTT}$ ) of 10 blanks (ultra-pure water)  
231 before and after optimization. As shown in Figure 3, before the system optimization,  
232 we found that the average  $\Delta\text{DTT}$  measured by 10 blanks was  $0.25\pm 0.04 \text{ nmol min}^{-1}$ ,  
233 and there is a big fluctuation. After optimization, the average  $\Delta\text{DTT}$  is  $0.14\pm 0.008 \text{ nmol}$   
234  $\text{min}^{-1}$ . It shows that air and light do promote the generation of ROS, and the nitrogen  
235 environment and avoiding light contribute to the stability of the system. The optimized  
236 system is more accurate in measuring the oxidation potential of environmental  
237 particulate matter. To further prove the optimization effect, the performance of the  
238 instrument is studied. (See Sect.3.1.4 for details)

#### 239 **3.1.2 Calibration of DTT<sub>v</sub> measurement and analysis system**

240 In past studies, PQN is often used as a standard sample of atmospheric particulate  
241 matter (Charrier and Anastasio, 2011; Charrier and Anastasio, 2015; Xiong et al., 2017).  
242 At pH 7.0, almost 100% of DTT was transformed to DTT-Disulfide by the catalyst 9,10-  
243 PQ (Li et al., 2009). The analytical measurement part of the online DTT instrument is  
244 calibrated by measuring the DTT activity of PQN at different concentrations. As shown  
245 in Figure 4, the linear graph of DTT consumption rate and PQN concentration, which  
246 is after subtracting the blank DTT consumption rate. The online detection slope is  
247  $3.66\pm 0.26$ , and the coefficient  $R^2=0.992$ . During the on-site operation, PQN's online  
248 and offline testing is measured at least once a month to ensure online accuracy.

#### 249 **3.1.3 Limit of detection and precision**

250 The limit of detection (LOD) of the system is defined as 3 times the standard  
251 deviation of the deionized water blank ( $N = 23$ ), i.e.,  $0.024 \text{ nmol min}^{-1}$ , which is  
252 significantly lower than the LOD of Puthussery et al. ( $0.24 \text{ nmol min}^{-1}$ ) and Fang et al.  
253 ( $0.31 \text{ nmol}\cdot\text{min}^{-1}$ ) (Fang et al., 2014; Puthussery et al., 2018). To ensure the accuracy  
254 of the system, the deionized water blank samples are taken once a day (14 days) during  
255 the sampling period, besides the 10 continuously measured during the optimization of  
256 the system.

257 Use deionized water to evaluate the accuracy of the environmental sample  
258 automation system and analyze the DTT activity. The low standard deviation  
259 (coefficient of variation, CV=5.61%) of 0.024 nmol min<sup>-1</sup> indicates that the system has  
260 sufficiently high accuracy for environmental samples.

#### 261 **3.1.4 Accuracy**

262 The accuracy of the system is verified by comparing the DTT activity of the  
263 positive control and environmental particulate samples obtained from the automated  
264 method with the results obtained from the same experimental protocol performed  
265 manually. (Cho et al., 2005)

266 Five concentrations of PQN solutions (0.01, 0.02, 0.025, 0.05, 0.085 nmol L<sup>-1</sup>) are  
267 run in the automatic system, which is very close to the results of the manual system (the  
268 standard deviation of the automatic system is kept at 0.008 nmol min<sup>-1</sup>, and the  
269 coefficient of variation is 2.28 %; the standard of the manual system The difference is  
270 0.0044 nmol min<sup>-1</sup>, the coefficient of variation is 1.48 %). As shown in Figure 5, the  
271 slope (manual/automatic) obtained by orthogonal fitting is 1.14, the intercept is 0.12,  
272 and the correlation coefficient (R<sup>2</sup>) is 0.997. The manual detection results are slightly  
273 higher than the automatic detection results, we assume that this is due to the instrument  
274 error caused by the complicated piping system of the online instrument. To ensure the  
275 high accuracy of the online system and the offline system, as a further verification, we  
276 used online and offline manual methods to conduct DTT activity analysis on ten  
277 environmental particulate matter samples.

278 As shown in Figure 6, the online and offline analysis of the DTT activity of 10  
279 ambient particles, the slope (manual/automatic) obtained by orthogonal fitting is 1.14,  
280 the intercept is 0.19, and the correlation coefficient (R<sup>2</sup>) is 0.954. We found that the real  
281 samples tested also had slightly higher offline results than online results. This is similar  
282 to our assumption. Therefore, we use the PQN online and offline DTT consumption  
283 rate orthogonal fitting result as the system to correct the error, as shown in Figure 6,  
284 through the offline and online orthogonal fitting of 10 environmental particulate matter  
285 samples before and after the error correction. We found that the corrected results are  
286 better (the slope is 0.97 closer to 1, the intercept is 0.05 closer to 0, R<sup>2</sup>=0.954). The  
287 good agreement between the two sampling systems indicates that the DTT  
288 measurement of environmental samples has high overall accuracy. These tests also  
289 proved the necessity of optimization.

#### 290 **3.2 DTT activity of ambient samples**

291 The volume-normalized oxidation potential DTT<sub>v</sub> is used as an index of exposure  
292 to inhaled air to point out the inherent ability of particles to deplete relevant antioxidants.  
293 During the observation period, the daily change of DTT<sub>v</sub> in Nanjing is shown in Figure  
294 7. The average DTT<sub>v</sub> is 0.83±0.38 nmol min<sup>-1</sup> m<sup>-3</sup>. Compared with Beijing's DTT<sub>v</sub> in  
295 the spring of 2012 (urban area: 0.24 nmol min<sup>-1</sup> m<sup>-3</sup>)(Liu et al., 2014; Wang et al., 2019).  
296 and Zhejiang University's annual DTT<sub>v</sub> average of 0.62 nmol min<sup>-1</sup> m<sup>-3</sup>(Yu et al., 2019) ,  
297 our results are on the high side; And compared with Peking University's 2015 annual  
298 DTT<sub>v</sub> (12.26±6.82 nmol min<sup>-1</sup> m<sup>-3</sup>) (Perrone et al., 2016) and Guangzhou's In the winter  
299 of 2017 (DTT<sub>v</sub>: 4.67±1.06 nmol min<sup>-1</sup> m<sup>-3</sup>) and in the spring of 2018 (DTT<sub>v</sub>: 4.45±1.02  
300 nmol min<sup>-1</sup> m<sup>-3</sup>), our values are low, which may be related to the current season and

301 emission factors. In addition, we found that the rain during the sampling period caused  
302 significant changes in the 24-hour DTT<sub>v</sub>. To better understand the environmental  
303 factors affecting DTT<sub>v</sub>, hourly data obtained by running the instrument is composited  
304 to obtain a diurnal profile of the DTT activity. As shown in Figure S2, the daily  
305 distribution of 24-hour DTT activities during the entire sampling period (a), before rain  
306 (b), during rain (c), and after rain (d) are divided. Figure S2(a) represents the hourly  
307 change of DTT<sub>v</sub> during the entire sample period. We found that the highest value of  
308 DTT<sub>v</sub> in a day occurs at 11-12 am, and DTT<sub>v</sub> is greater during the day than at night,  
309 which is similar to the study by Puthussery et al. Before the rain, the average DTT<sub>v</sub> was  
310  $0.81 \pm 0.17 \text{ nmol min}^{-1} \text{ m}^{-3}$ . There is a peak at 10-12 am, but the overall situation is  
311 relatively flat, and there is no obvious difference between day and night. And the  
312 average value of DTT<sub>v</sub> during the rain is  $0.55 \pm 0.10 \text{ nmol min}^{-1} \text{ m}^{-3}$ , which decreased  
313 significantly. There is no doubt that this is caused by rain settling the polluting  
314 components of the atmosphere. In contrast, there is significant daily activity in DTT<sub>v</sub>  
315 following rain, with peaks occurring mainly between 8-10 am and 4-6 pm, and DTT<sub>v</sub>  
316 is significantly higher during the day than at night, which is similar to the Puthussery  
317 study (Puthussery et al., 2018). However, there are no obvious diurnal variation in PM<sub>2.5</sub>  
318 mass concentration. Therefore, the diurnal variation of DTT activity is assumed to be  
319 mainly attributed from different emission sources at the site.

### 320 **3.3 The correlation between PM<sub>2.5</sub> and polluting gases and ROS activity**

321 To further study, the daily changes of DTT<sub>v</sub> and its correlation with various  
322 emission sources on site. As shown in Figure 7, we measured the water-soluble ionic  
323 components of PM<sub>2.5</sub> (SO<sub>4</sub><sup>2-</sup>, NO<sub>3</sub><sup>-</sup>, NH<sub>4</sub><sup>+</sup>, Na<sup>+</sup>, Ca<sup>2+</sup>, K<sup>+</sup>), BC, and pollution gas (SO<sub>2</sub>,  
324 CO, O<sub>3</sub>, NH<sub>3</sub>) content changes. The average concentration of PM<sub>2.5</sub> during the sampling  
325 period is  $9.97 \pm 6.53 \text{ ug m}^{-3}$ , the average concentration of PM<sub>2.5</sub> before rain is  $11.13 \pm 7.21$   
326  $\text{ug m}^{-3}$ , the average concentration of PM<sub>2.5</sub> after rain is  $7.80 \pm 4.18 \text{ ug m}^{-3}$ . The  
327 concentration of PM<sub>2.5</sub> is a significant drop. In addition, as shown in Table 1, there are  
328 differences in the correlation between PM<sub>2.5</sub> and DTT<sub>v</sub> before and after rain. Therefore,  
329 we suspect that the source of DTT<sub>v</sub> is different before and after the rain. BC and the  
330 polluting gases SO<sub>2</sub>, NO<sub>x</sub>, NO<sub>2</sub>, CO, Ca<sup>2+</sup>, K<sup>+</sup>, Mg<sup>2+</sup> are often used as tracers of biomass  
331 burning, coal combustion, and dust storms. Compared with the early winter in the  
332 northern suburbs of Nanjing (Zhang et al., 2020), the levels of these substances  
333 decreased during the sampling period. It is similar to Liu and Zhang et al who concluded  
334 that biomass burning, coal combustion, and dust storms were not major sources of  
335 pollution in Nanjing during the summer (Guo et al., 2019; Liu et al., 2019; Zhang et al.,  
336 2020). In addition, there is no strong correlation between DTT<sub>v</sub> and SO<sub>2</sub>, NO<sub>x</sub>, NO<sub>2</sub>,  
337 and CO before and after the rain. Therefore, it can be judged that neither biomass  
338 burning, coal combustion nor dust is the main source affecting DTT<sub>v</sub>. In contrast, we  
339 found that there is a significant difference between day and night in O<sub>3</sub> after rain, which  
340 is similar to the change of DTT<sub>v</sub>, and after rain, DTT<sub>v</sub> and O<sub>3</sub> show a strong correlation  
341 ( $r=0.624$ ). After it rains, the O<sub>3</sub> content in the air environment increases. Under the  
342 action of the sun's ultraviolet rays, the O<sub>3</sub> is photodegraded to form active oxygen  
343 components such as OH radicals (Ehhalt and Rohrer, 2000; Rohrer and Berresheim,  
344 2006).



345 To further confirm the influence of light on DTT<sub>v</sub>, the day and night correlation  
346 analysis of substances related to photo-oxidation (NH<sub>4</sub><sup>+</sup>, NO<sub>3</sub><sup>-</sup>, SO<sub>4</sub><sup>2-</sup>) and DTT<sub>v</sub> is  
347 carried out. As shown in Table S2, we find that NH<sub>4</sub><sup>+</sup>, NO<sub>3</sub><sup>-</sup>, SO<sub>4</sub><sup>2-</sup> and DTT<sub>v</sub> are  
348 significantly correlated during the day (r=0.434, r=0.461, r=0.263, P<0.01). As far as  
349 we know, there is no evidence in the literature that water-soluble inorganic ions (NH<sub>4</sub><sup>+</sup>,  
350 NO<sub>3</sub><sup>-</sup>, SO<sub>4</sub><sup>2-</sup>) have redox activity in an aerobic environment (Calas et al., 2018;  
351 Stevanovic et al., 2017). However, their correlation with DTT<sub>v</sub> may be due to  
352 collinearity with redox-active organic compounds, rather than actual contribution to the  
353 oxidation potential of particles. We speculate that the high correlation may be related  
354 to the photochemical reactions that occur during the day.

#### 355 **4、 Summary and conclusions**

356 This study proposes and characterizes an improved online active oxygen analyzer.  
357 Compared with the previous research, the main improvements (Fang et al., 2014;  
358 Puthussery et al., 2018). The optimization analysis is as follows: (1) The experimental  
359 environment is processed to isolate the air and avoid light; (2) The sampling method  
360 has changed. We use the MARGA online ion analyzer, which is more mature and stable.  
361 Compared with before optimization, the standard deviation of the blank was  
362 significantly smaller. Thus, the detection limit of the instrument (0.024 nmol min<sup>-1</sup>)  
363 becomes smaller and more stable. The DTT consumption rate is reduced by 44 %,  
364 which eliminates the influence of outside air and light in the experiment. And the  
365 consistency between online and offline is improved (slope=0.97, R<sup>2</sup>=0.95), the  
366 accuracy of the system is higher.

367 By changing the DTT<sub>v</sub> content hour by hour during the sampling period, we found  
368 that the DTT activity during the day is higher than that at night, and it is especially  
369 obvious after rain, which is mainly related to the increase in UV radiation during the  
370 day after rain. In addition, we analyzed the correlation between water-soluble ions  
371 (SO<sub>4</sub><sup>2-</sup>, NO<sub>3</sub><sup>-</sup>, NH<sub>4</sub><sup>+</sup>, Na<sup>+</sup>, Ca<sup>2+</sup>, K<sup>+</sup>), BC, pollutant gases (SO<sub>2</sub>, CO, O<sub>3</sub>, NO, NO<sub>x</sub>, NH<sub>3</sub>)  
372 and DTT<sub>v</sub>, and we found that the main source of influence of OP in the Nanjing  
373 environment in summer is daytime Secondary photochemical conversion and  
374 ultraviolet radiation. In the future, we hope to add more experimental modules to the  
375 back-end based on the MARGA sample collection device to realize the diversification  
376 of detection compositions. In addition, the system can be combined with other  
377 substance detection instruments. It will achieve the daily contribution of various  
378 emission sources to the risk associated with OP exposure can be inferred from other  
379 species.

380

381 *Data availability.* Data used in this paper can be provided upon request by email to  
382 ZYL (dryanlinzhang@outlook.com) .

383 *Author contributions.* WJY designed the instrument, led the sampling campaign,  
384 performed the experiments, and wrote the manuscript. YC participated in experimental  
385 design and guided the experimental process. ZCY chose the building address and  
386 initially built the instrument. CF helped in the filter collection and in conducting the  
387 DTT activity experiments. ZYL conceived the idea, organized the manuscript, and  
388 supervised the project.

389 *Competing interests.* The authors declare that they have no conflict of interest.

390 *Acknowledgements.* The authors thank funding support from the National Nature  
391 Science Foundation of China (Nos. 41977305), the Natural Science Foundation of  
392 Jiangsu Province (No. BK20180040), the fund from Jiangsu Innovation &  
393 Entrepreneurship Team.

394

395 **References:**

- 396 Ahmad, M., Yu, Q., Chen, J., Cheng, S., Qin, W., and Zhang, Y.: Chemical characteristics, oxidative  
397 potential, and sources of PM (2.5) in wintertime in Lahore and Peshawar, Pakistan, *J Environ Sci*  
398 (China), 102, 148-158, <https://doi.org/10.1016/j.jes.2020.09.014>, 2021.
- 399 Akhtar, U. S., McWhinney, R. D., Rastogi, N., Abbatt, J. P., Evans, G. J., and Scott, J. A.: Cytotoxic and  
400 proinflammatory effects of ambient and source-related particulate matter (PM) in relation to the  
401 production of reactive oxygen species (ROS) and cytokine adsorption by particles, *Inhal Toxicol*, 22  
402 Suppl 2, 37-47, <https://doi.org/10.3109/08958378.2010.518377>, 2010.
- 403 Ayres, J. G., Borm, P., Cassee, F. R., Castranova, V., Donaldson, K., Ghio, A., Harrison, R. M., Hider, R.,  
404 Kelly, F., Kooter, I. M., Marano, F., Maynard, R. L., Mudway, I., Nel, A., Sioutas, C., Smith, S., Baeza-  
405 Squiban, A., Cho, A., Duggan, S., and Froines, J.: Evaluating the toxicity of airborne particulate matter  
406 and nanoparticles by measuring oxidative stress potential--a workshop report and consensus statement,  
407 *Inhal Toxicol*, 20, 75-99, <https://doi.org/10.1080/08958370701665517>, 2008.
- 408 Bates, J. T., Fang, T., Verma, V., Zeng, L., Weber, R. J., Tolbert, P. E., Abrams, J. Y., Sarnat, S. E., Klein,  
409 M., Mulholland, J. A., and Russell, A. G.: Review of Acellular Assays of Ambient Particulate Matter  
410 Oxidative Potential: Methods and Relationships with Composition, Sources, and Health Effects, *Environ.*  
411 *Sci. Technol.*, 53, 4003-4019, <https://doi.org/10.1021/acs.est.8b03430>, 2019.
- 412 Borm, P. J. A., Kelly, F., Künzli, N., Schins, R. P. F., and Donaldson, K.: Oxidant generation by particulate  
413 matter: from biologically effective dose to a promising, novel metric, *Occup Environ Med*, 64, 73-74,  
414 <https://doi.org/10.1136/oem.2006.029090>, 2007.
- 415 Calas, A., Uzu, G., Kelly, F. J., Houdier, S., Martins, J. M. F., Thomas, F., Molton, F., Charron, A., Dunster,  
416 C., Oliete, A., Jacob, V., Besombes, J. L., Chevrier, F., and Jaffrezo, J. L.: Comparison between five  
417 acellular oxidative potential measurement assays performed with detailed chemistry on PM10 samples  
418 from the city of Chamonix (France), *Atmos. Chem. Phys.*, 18, 7863-7875, [https://doi.org/10.5194/acp-](https://doi.org/10.5194/acp-18-7863-2018)  
419 [18-7863-2018](https://doi.org/10.5194/acp-18-7863-2018), 2018.
- 420 Charrier, J. G. and Anastasio, C.: Impacts of Antioxidants on Hydroxyl Radical Production from  
421 Individual and Mixed Transition Metals in a Surrogate Lung Fluid, *Atmospheric Environ. (Oxford,*  
422 *England : 1994)*, 45, 7555-7562, <https://doi.org/10.1016/j.atmosenv.2010.12.021>, 2011.
- 423 Charrier, J. G. and Anastasio, C.: Rates of Hydroxyl Radical Production from Transition Metals and  
424 Quinones in a Surrogate Lung Fluid, *Environ. Sci. Technol.*, 49, 9317-9325,  
425 <https://doi.org/10.1021/acs.est.5b01606>, 2015.
- 426 Charrier, J. G., McFall, A. S., Vu, K. K. T., Baroi, J., Olea, C., Hasson, A., and Anastasio, C.: A bias in  
427 the “mass-normalized” DTT response – An effect of non-linear concentration-response curves for copper  
428 and manganese, *Atmospheric Environ.*, 144, 325-334, <https://doi.org/10.1016/j.atmosenv.2016.08.071>,  
429 2016.
- 430 Chen, X., Walker, J. T., and Geron, C.: Chromatography related performance of the Monitor for AeRosols  
431 and GAses in ambient air (MARGA): laboratory and field-based evaluation, *Atmos. Meas. Tech.*, 10,  
432 3893-3908, [10.5194/amt-10-3893-2017](https://doi.org/10.5194/amt-10-3893-2017), 2017.
- 433 Chen, X., Zhong, Z., Xu, Z., Chen, L., and Wang, Y.: 2',7'-Dichlorodihydrofluorescein as a fluorescent  
434 probe for reactive oxygen species measurement: Forty years of application and controversy, *Free Radic*  
435 *Res*, 44, 587-604, <https://doi.org/10.3109/10715761003709802>, 2010.
- 436 Cho, A. K., Sioutas, C., Miguel, A. H., Kumagai, Y., Schmitz, D. A., Singh, M., Eiguren-Fernandez, A.,  
437 and Froines, J. R.: Redox activity of airborne particulate matter at different sites in the Los Angeles Basin,  
438 *Environ. Res.*, 99, 40-47, <https://doi.org/10.1016/j.envres.2005.01.003>, 2005.

439 Delfino, R. J., Sioutas, C., and Malik, S.: Potential role of ultrafine particles in associations between  
440 airborne particle mass and cardiovascular health, *Environ. Health Perspect.*, 113, 934-946,  
441 <https://doi.org/10.1289/ehp.7938>, 2005.

442 Delfino, R. J., Staimer, N., Tjoa, T., Gillen, D. L., Schauer, J. J., and Shafer, M. M.: Airway inflammation  
443 and oxidative potential of air pollutant particles in a pediatric asthma panel, *J Expo Sci Environ  
444 Epidemiol*, 23, 466-473, <https://doi.org/10.1038/jes.2013.25>, 2013.

445 Dou, J., Lin, P., Kuang, B.-Y., and Yu, J.: Reactive Oxygen Species Production Mediated by Humic-like  
446 Substances in Atmospheric Aerosols: Enhancement Effects by Pyridine, Imidazole, and Their  
447 Derivatives, *Environ. Sci. Technol.*, 49, <https://doi.org/10.1021/es5059378>, 2015.

448 Ehhalt, D. H. and Rohrer, F.: Dependence of the OH concentration on solar UV, *J. Geophys. Res.:  
449 Atmospheres*, 105, 3565-3571, <https://doi.org/10.1029/1999jd901070>, 2000.

450 Eiguren-Fernandez, A., Kreisberg, N., and Hering, S.: An online monitor of the oxidative capacity of  
451 aerosols (o-MOCA), *Atmos Meas Tech*, 10, 633-644, <https://doi.org/10.5194/amt-10-633-2017>, 2017.

452 Fang, T., Guo, H., Zeng, L., Verma, V., Nenes, A., and Weber, R. J.: Highly Acidic Ambient Particles,  
453 Soluble Metals, and Oxidative Potential: A Link between Sulfate and Aerosol Toxicity, *Environ. Sci.  
454 Technol.*, 51, 2611-2620, <https://doi.org/10.1021/acs.est.6b06151>, 2017.

455 Fang, T., Verma, V., Guo, H., King, L., Edgerton, E., and Weber, R.: A semi-automated system for  
456 quantifying the oxidative potential of ambient particles in aqueous extracts using the dithiothreitol (DTT)  
457 assay: Results from the Southeastern Center for Air Pollution and Epidemiology (SCAPE), *Atmos Meas  
458 Tech Discussions*, 7, 7245-7279, <https://doi.org/10.5194/amtd-7-7245-2014>, 2014.

459 Fang, T., Verma, V., Bates, J., Abrams, J., Strickland, M., Ebel, S., Chang, H., Mulholland, J., Tolbert,  
460 P., Russell, A., and Weber, R.: Oxidative potential of ambient water-soluble PM<sub>2.5</sub> in the  
461 southeastern United States: contrasts in sources and health associations between ascorbic acid (AA) and  
462 dithiothreitol (DTT) assays, *Atmospheric Chem. Phys.*, 16, <https://doi.org/10.5194/acp-16-3865-2016>,  
463 2016.

464 Ghio, A. J., Carraway, M. S., and Madden, M. C.: Composition of air pollution particles and oxidative  
465 stress in cells, tissues, and living systems, *J. Toxicol. Environ. Health. Part B, Critical reviews*, 15, 1-21,  
466 <https://doi.org/10.1080/10937404.2012.632359>, 2012.

467 Guo, Z., Guo, Q., Chen, S., Zhu, B., Zhang, Y., Yu, J., and Guo, Z.: Study on pollution behavior and  
468 sulfate formation during the typical haze event in Nanjing with water soluble inorganic ions and sulfur  
469 isotopes, *Atmos Res*, 217, 198-207, <https://doi.org/10.1016/j.atmosres.2018.11.009>, 2019.

470 Hedayat, F., Stevanovic, S., Miljevic, B., Bottle, S., and Ristovski, Z.: Review – Evaluating the molecular  
471 assays for measuring the oxidative potential of particulate matter, *Chem Ind Chem Engg*, 21, 31-31,  
472 <https://doi.org/10.2298/CICEQ140228031H>, 2014.

473 Hellack, B., Quass, U., Nickel, C., Wick, G., Schins, R. P. F., and Kuhlbusch, T. A. J.: Oxidative potential  
474 of particulate matter at a German motorway, *Environ Sci Process Impacts*, 17, 868-876,  
475 <https://doi.org/10.1039/c4em00605d>, 2015.

476 Hemmilä, M., Hellén, H., Virkkula, A., Makkonen, U., Praplan, A. P., Kontkanen, J., Ahonen, L.,  
477 Kulmala, M., and Hakola, H.: Amines in boreal forest air at SMEAR II station in Finland, *Atmospheric  
478 Chem. Phys.*, 18, 6367-6380, [10.5194/acp-18-6367-2018](https://doi.org/10.5194/acp-18-6367-2018), 2018.

479 Huang, W., Zhang, Y., Zhang, Y., Zeng, L., Dong, H., Huo, P., Fang, D., and Schauer, J. J.: Development  
480 of an automated sampling-analysis system for simultaneous measurement of reactive oxygen species  
481 (ROS) in gas and particle phases: GAC-ROS, *Atmospheric Environ.*, 134, 18-26,  
482 <https://doi.org/10.1016/j.atmosenv.2016.03.038>, 2016.

483 Janssen, N. A., Strak, M., Yang, A., Hellack, B., Kelly, F. J., Kuhlbusch, T. A., Harrison, R. M.,  
484 Brunekreef, B., Cassee, F. R., Steenhof, M., and Hoek, G.: Associations between three specific a-cellular  
485 measures of the oxidative potential of particulate matter and markers of acute airway and nasal  
486 inflammation in healthy volunteers, *Occup Environ Med*, 72, 49-56, [https://doi.org/10.1136/oemed-](https://doi.org/10.1136/oemed-2014-102303)  
487 2014-102303, 2015.

488 Li, Q., Wyatt, A., and Kamens, R. M.: Oxidant generation and toxicity enhancement of aged-diesel  
489 exhaust, *Atmospheric Environ.*, 43, 1037-1042, 10.1016/j.atmosenv.2008.11.018, 2009.

490 Li, Y., Zhu, T., Zhao, J., and Xu, B.: Interactive enhancements of ascorbic acid and iron in hydroxyl  
491 radical generation in quinone redox cycling, *Environ. Sci. Technol.*, 46, 10302-10309,  
492 <https://doi.org/10.1021/es301834r>, 2012.

493 Lin, M. and Yu, J. Z.: Dithiothreitol (DTT) concentration effect and its implications on the applicability  
494 of DTT assay to evaluate the oxidative potential of atmospheric aerosol samples, *Environ Pollut*, 251,  
495 938-944, 10.1016/j.envpol.2019.05.074, 2019.

496 Liu, Q., Baumgartner, J., Zhang, Y., Liu, Y., Sun, Y., and Zhang, M.: Oxidative potential and  
497 inflammatory impacts of source apportioned ambient air pollution in Beijing, *Environ. Sci. Technol.*, 48,  
498 12920-12929, 10.1021/es5029876, 2014.

499 Liu, X., Zhang, Y. L., Peng, Y., Xu, L., Zhu, C., Cao, F., Zhai, X., Haque, M. M., Yang, C., Chang, Y.,  
500 Huang, T., Xu, Z., Bao, M., Zhang, W., Fan, M., and Lee, X.: Chemical and optical properties of  
501 carbonaceous aerosols in Nanjing, eastern China: regionally transported biomass burning contribution,  
502 *Atmos. Chem. Phys.*, 19, 11213-11233, <https://doi.org/10.5194/acp-19-11213-2019>, 2019.

503 Lodovici, M. and Bigagli, E.: Oxidative stress and air pollution exposure, *J. Toxicol*, 2011, 487074,  
504 <https://doi.org/10.1155/2011/487074>, 2011.

505 Pal, A. K., Bello, D., Budhlall, B., Rogers, E., and Milton, D. K.: Screening for Oxidative Stress Elicited  
506 by Engineered Nanomaterials: Evaluation of Acellular DCFH Assay, *Dose Response*, 10, 308-330,  
507 <https://doi.org/10.2203/dose-response.10-036.Pal>, 2012.

508 Perrone, M. G., Zhou, J., Malandrino, M., Sangiorgi, G., Rizzi, C., Ferrero, L., Dommen, J., and  
509 Bolzacchini, E.: PM chemical composition and oxidative potential of the soluble fraction of particles at  
510 two sites in the urban area of Milan, Northern Italy, *Atmospheric Environ.*, 128, 104-113,  
511 <https://doi.org/10.1016/j.atmosenv.2015.12.040>, 2016.

512 Pöschl, U. and Shiraiwa, M.: Multiphase chemistry at the atmosphere-biosphere interface influencing  
513 climate and public health in the anthropocene, *Chemical reviews*, 115, 4440-4475,  
514 <https://doi.org/10.1021/cr500487s>, 2015.

515 Puthussery, J. V., Zhang, C., and Verma, V.: Development and field testing of an online instrument for  
516 measuring the real-time oxidative potential of ambient particulate matter based on dithiothreitol assay,  
517 *Atmos. Meas. Tech.*, 11, 5767-5780, <https://doi.org/10.5194/amt-11-5767-2018>, 2018.

518 Rohrer, F. and Berresheim, H.: Strong correlation between levels of tropospheric hydroxyl radicals and  
519 solar ultraviolet radiation, *Nature*, 442, 184-187, <https://doi.org/10.1038/nature04924>, 2006.

520 Sameenoi, Y., Koehler, K., Shapiro, J., Boonsong, K., Sun, Y., Collett, J., Jr., Volckens, J., and Henry, C.  
521 S.: Microfluidic electrochemical sensor for on-line monitoring of aerosol oxidative activity, *J. Am. Chem.*  
522 *Soc.*, 134, 10562-10568, <https://doi.org/10.1021/ja3031104>, 2012.

523 Stevanovic, S., Vaughan, A., Hedayat, F., Salimi, F., Rahman, M. M., Zare, A., Brown, R. A., Brown, R.  
524 J., Wang, H., Zhang, Z., Wang, X., Bottle, S. E., Yang, I. A., and Ristovski, Z. D.: Oxidative potential of  
525 gas phase combustion emissions - An underestimated and potentially harmful component of air pollution  
526 from combustion processes, *Atmospheric Environ.*, 158, 227-235,

527 <https://doi.org/10.1016/j.atmosenv.2017.03.041>, 2017.

528 Stieger, B., Spindler, G., van Pinxteren, D., Grüner, A., Wallasch, M., and Herrmann, H.: Development  
529 of an online-coupled MARGA upgrade for the 2&thinsp;h interval quantification of low-molecular-  
530 weight organic acids in the gas and particle phases, *Atmos. Meas. Tech.*, 12, 281-298,  
531 <https://doi.org/10.5194/amt-12-281-2019>, 2019.

532 Velali, E., Papachristou, E., Pantazaki, A., Choli-Papadopoulou, T., Planou, S., Kouras, A., Manoli, E.,  
533 Besis, A., Voutsas, D., and Samara, C.: Redox activity and in vitro bioactivity of the water-soluble fraction  
534 of urban particulate matter in relation to particle size and chemical composition, *Environ. Pollut.*, 208,  
535 774-786, <https://doi.org/10.1016/j.envpol.2015.10.058>, 2016.

536 Visentin, M., Pagnoni, A., Sarti, E., and Pietrogrande, M. C.: Urban PM<sub>2.5</sub> oxidative potential: Importance  
537 of chemical species and comparison of two spectrophotometric cell-free assays, *Environ. Pollut.*, 219,  
538 72-79, <https://doi.org/10.1016/j.envpol.2016.09.047>, 2016.

539 Vreeland, H., Weber, R., Bergin, M., Greenwald, R., Golan, R., Russell, A. G., Verma, V., and Sarnat, J.  
540 A.: Oxidative potential of PM<sub>2.5</sub> during Atlanta rush hour: Measurements of in-vehicle dithiothreitol  
541 (DTT) activity, *Atmospheric Environ.*, 165, 169-178, <https://doi.org/10.1016/j.atmosenv.2017.06.044>,  
542 2017.

543 Wang, J., Lin, X., Lu, L., Wu, Y., Zhang, H., Lv, Q., Liu, W., Zhang, Y., and Zhuang, S.: Temporal  
544 variation of oxidative potential of water soluble components of ambient PM<sub>2.5</sub> measured by dithiothreitol  
545 (DTT) assay, *Sci. Total Environ.*, 649, 969-978, <https://doi.org/10.1016/j.scitotenv.2018.08.375>, 2019.

546 Wragg, F. P. H., Fuller, S. J., Freshwater, R., Green, D. C., Kelly, F. J., and Kalberer, M.: An automated  
547 online instrument to quantify aerosol-bound reactive oxygen species (ROS) for ambient measurement  
548 and health-relevant aerosol studies, *Atmos. Meas. Tech.*, 9, 4891-4900, <https://doi.org/10.5194/amt-9-4891-2016>, 2016.

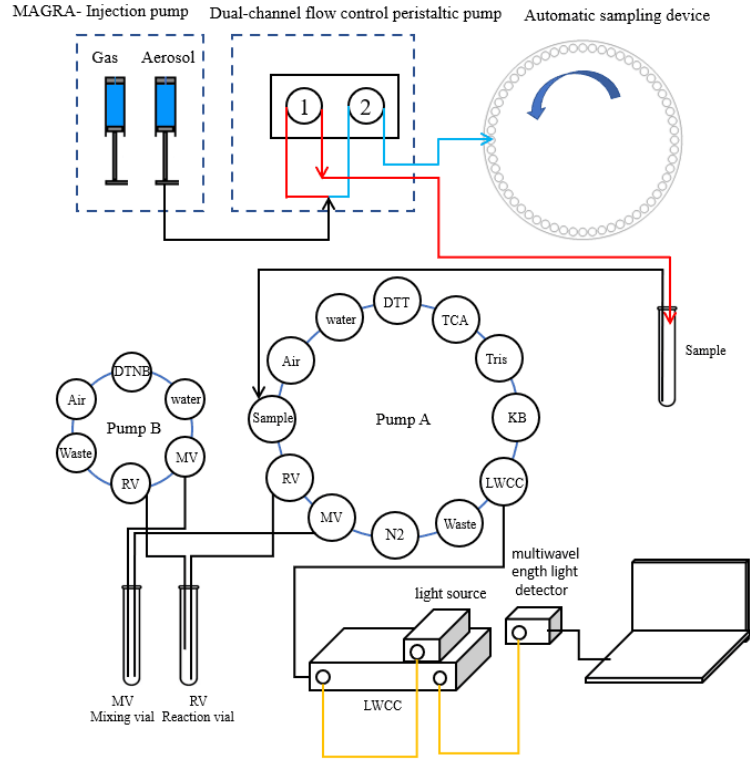
550 Xiong, Q., Yu, H., Wang, R., Wei, J., and Verma, V.: Rethinking Dithiothreitol-Based Particulate Matter  
551 Oxidative Potential: Measuring Dithiothreitol Consumption versus Reactive Oxygen Species Generation,  
552 *Environ. Sci. Technol.*, 51, 6507-6514, <https://doi.org/10.1021/acs.est.7b01272>, 2017.

553 Yang, A., Jedynska, A., Hellack, B., Kooter, I., Hoek, G., Brunekreef, B., Kuhlbusch, T. A. J., Cassee, F.  
554 R., and Janssen, N. A. H.: Measurement of the oxidative potential of PM<sub>2.5</sub> and its constituents: The effect  
555 of extraction solvent and filter type, *Atmospheric Environ.*, 83, 35-42,  
556 <https://doi.org/10.1016/j.atmosenv.2013.10.049>, 2014.

557 Yu, S., Liu, W., Xu, Y., Yi, K., Zhou, M., Tao, S., and Liu, W.: Characteristics and oxidative potential of  
558 atmospheric PM<sub>2.5</sub> in Beijing: Source apportionment and seasonal variation, *Sci. Total Environ.*, 650,  
559 277-287, <https://doi.org/10.1016/j.scitotenv.2018.09.021>, 2019.

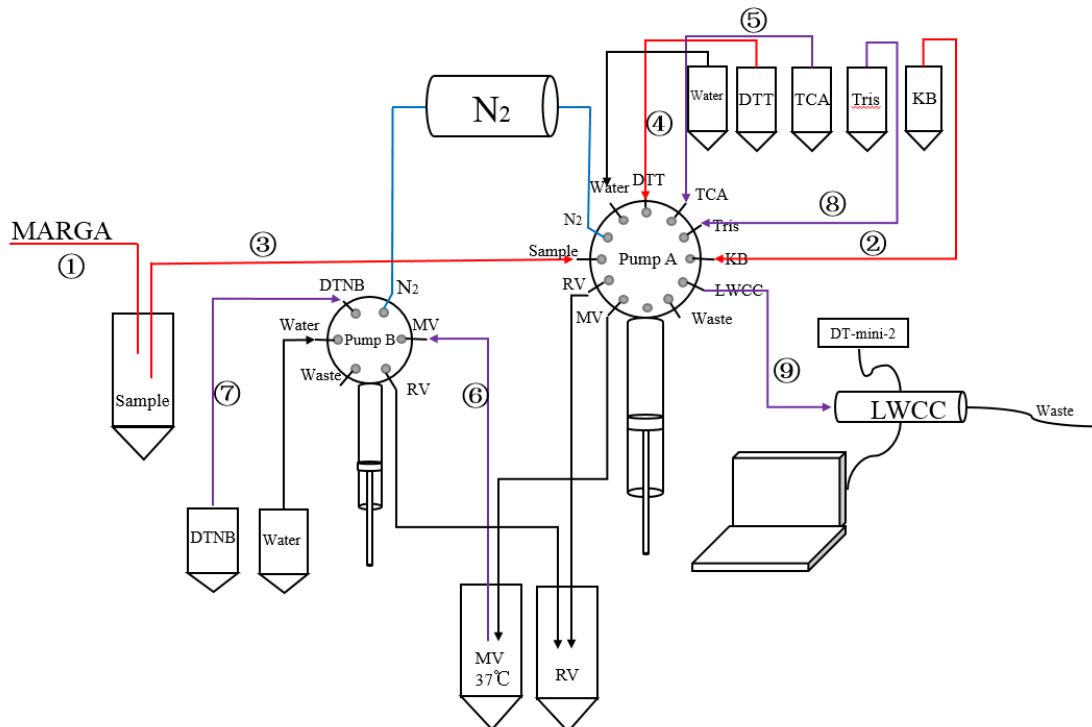
560 Zhang, C., Yang, C., Liu, X., Cao, F., and Zhang, Y.-l.: Insight into the photochemistry of atmospheric  
561 oxalate through hourly measurements in the northern suburbs of Nanjing, China, *Sci. Total Environ.*, 719,  
562 137416, <https://doi.org/10.1016/j.scitotenv.2020.137416>, 2020.

563



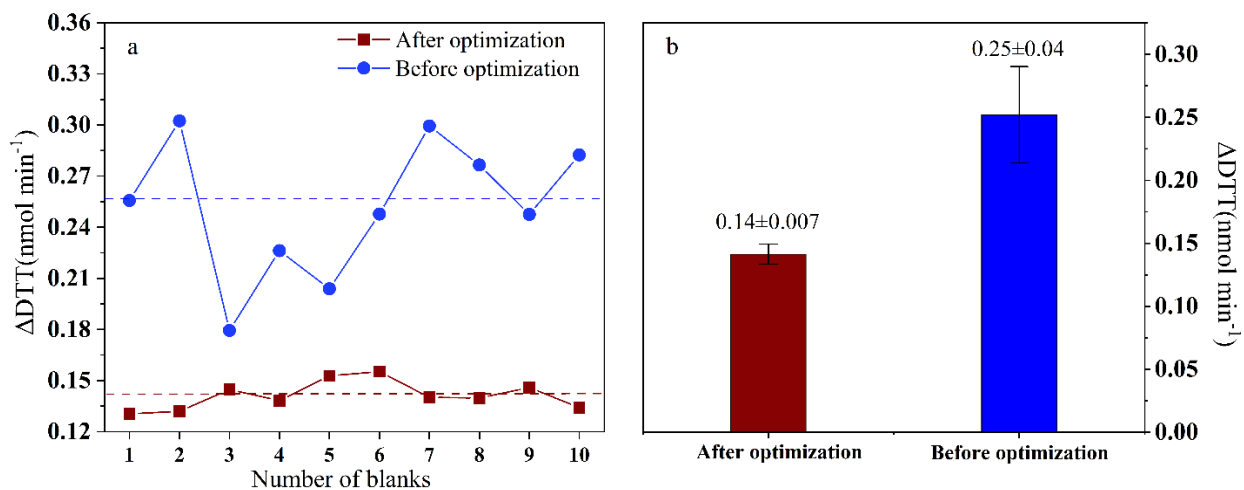
564

565 **Figure 1.** Automated system setup (Red line: Peristaltic pump 1 runs at a flow rate of 23 ml h<sup>-1</sup> for the first 4 minutes of each hour; Blue line: Peristaltic pump 2 runs at a flow rate of 27 ml h<sup>-1</sup> for the  
 566 remaining 56 minutes of each hour; Yellow line: Optical fiber)  
 567



568

569 **Figure 2** Schematic diagram of DTT reaction part. (①-④ represents the DTT oxidation step,⑤-⑨  
 570 represents the DTT determination step. Blue indicates the ventilation line, all pipelines are wrapped  
 571 in aluminum foil to protect from light.)

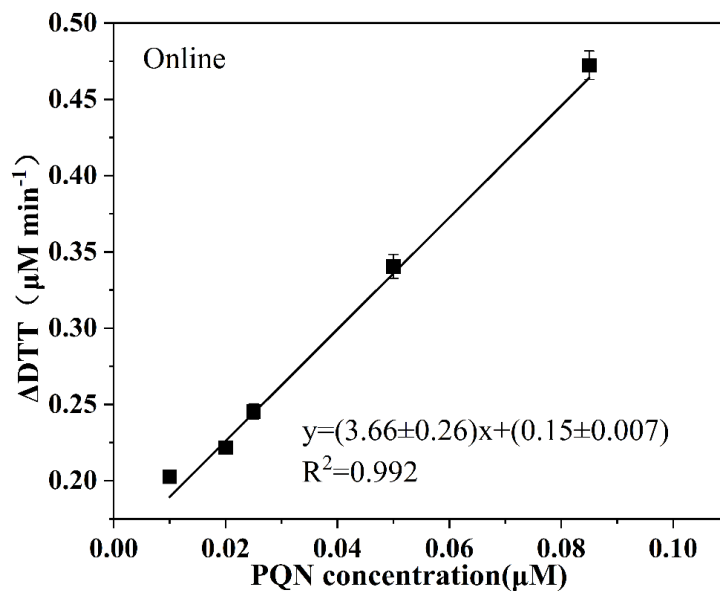


572

573

574

**Figure 3.** Comparison of blank DTT consumption rate and standard deviation after system optimization (the dotted line is the average value)



575

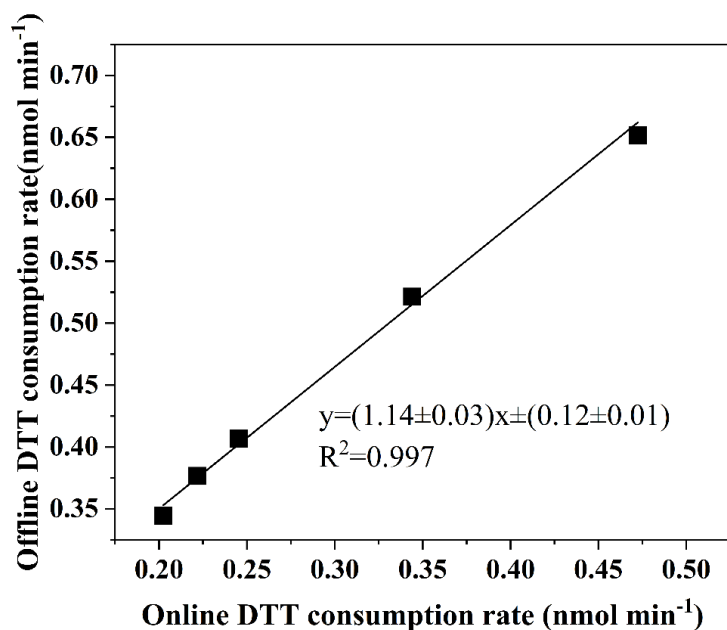
576

577

578

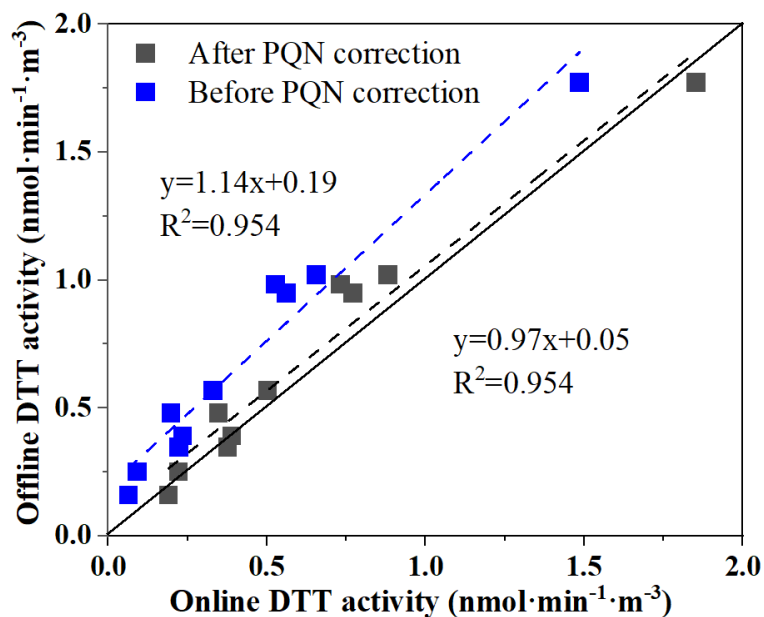
**Figure 4.** Blank corrected DTT consumption rate as a function of PQN used as a positive control. Each error bar represents the standard deviation of three independent DTT measurements on each concentration.





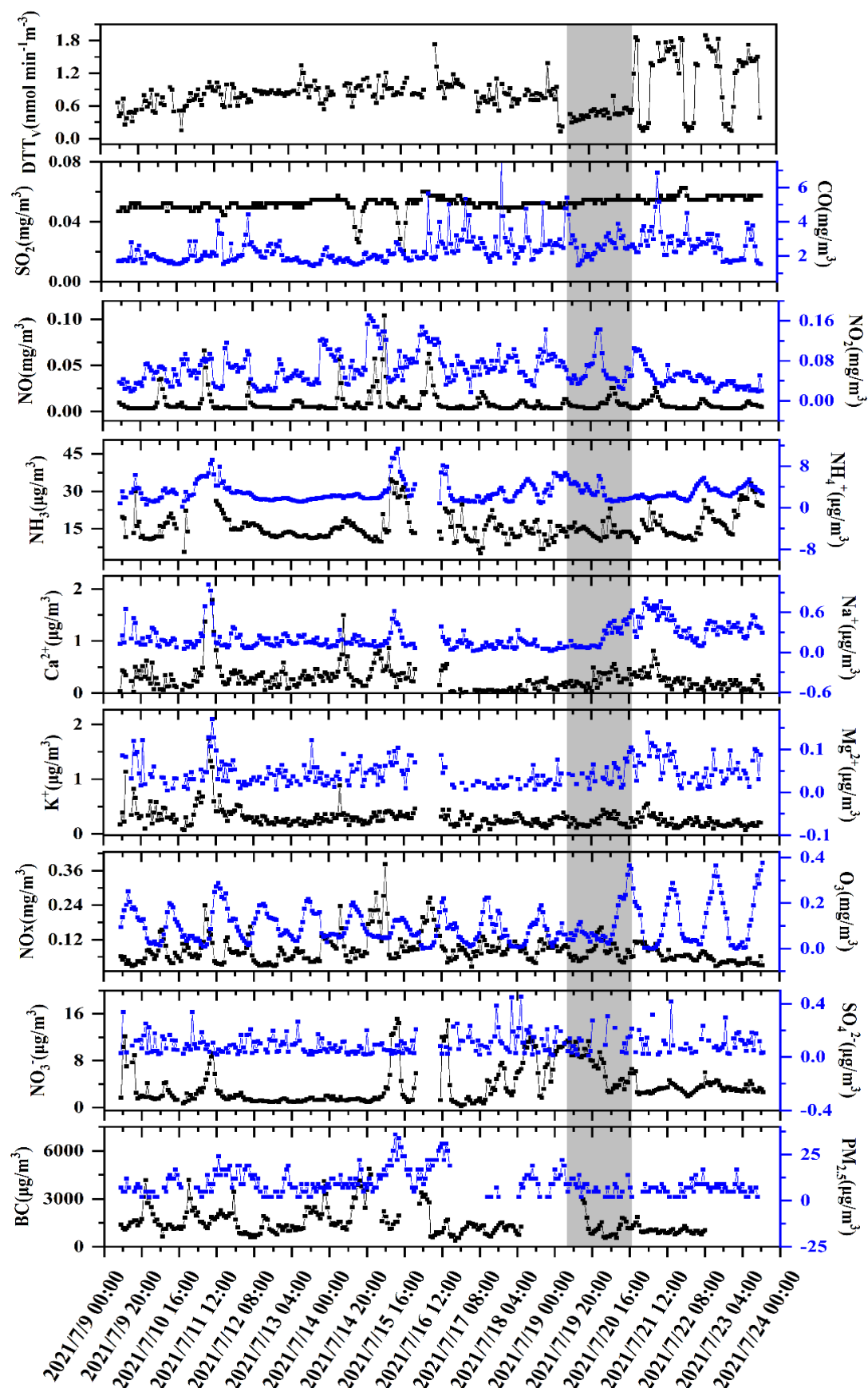
579

580 **Figure 5.** Comparison of the automated system with manual operation using PQN (9,10-  
 581 phenanthraquinone)



582

583 **Figure 6.** Comparison of the automated system with manual operation using ambient aerosol  
 584 extracts (PM<sub>2.5</sub> samples collected from Xuzhou, regression analysis is done by orthogonal  
 585 regression; the line is 1:1).  
 586



587

588

589

**Figure 7 .** Time series of the DTT activity, PM<sub>2.5</sub> water-soluble components (SO<sub>4</sub><sup>2-</sup>, NO<sub>3</sub><sup>-</sup>, NH<sub>4</sub><sup>+</sup>, Na<sup>+</sup>, Ca<sup>2+</sup>, K<sup>+</sup>) and polluting gases (SO<sub>2</sub>, CO, O<sub>3</sub>, NH<sub>3</sub>) (The shaded part is rainy weather)

590

591 **Table 1.** The correlation coefficient (R) between the concentration of water-soluble chemical  
 592 substances in environmental PM<sub>2.5</sub> ( $\mu\text{g m}^{-3}$ ) and the volume normalized substance concentration  
 593 (DTTV), before rain, during rain, and after rain.

Parameter	Total	Before it rains	During rain	After rain
PM <sub>2.5</sub>	0.014	0.305**	0.026	-0.290*
SO <sub>2</sub>	0.195**	0.114	-0.136	0.222
NO	-0.029	-0.029	-0.074	0.050
NO <sub>2</sub>	-0.098	0.115	0.169	-0.203
NO <sub>x</sub>	-0.085	0.062	0.142	-0.169
CO	-0.033	0.146*	-0.093	0.121
O <sub>3</sub>	0.227*	0.153	0.044	0.624**
BC	-0.052	-0.054	-0.439*	0.087
NH <sub>3</sub>	0.241**	0.074	-0.129	0.269*
SO <sub>4</sub> <sup>2-</sup>	-0.06	-0.065	0.329	0.028
NO <sub>3</sub> <sup>-</sup>	-0.163*	-0.155*	-0.352*	0.511**
NH <sub>4</sub> <sup>+</sup>	0.024	0.028	0.062	0.271*
K <sup>+</sup>	-0.077	-0.045	0.125	-0.337**
Mg <sup>2+</sup>	0.131*	0.075	0.233	0.086
Ca <sup>2+</sup>	0.005	0.072	0.021	-0.055
Na <sup>+</sup>	0.177**	-0.007	0.133	0.008

594

PM<sub>2.5</sub>, particulate matter with an aerodynamic diameter < 2.5 $\mu\text{m}$ ; \*P<0.05, \*\*P<0.01.

595